Table 1 Biased and unbiased two-component LDV data

	Biased data (2000 samples)	Unbiased data (2000 samples)
$\bar{U}$ m/s	28.0	27.99
$\bar{V}$ m/s	1.19	0.017
u' m/s	0.404	0.399
v' m/s	0.397	0.434
$\overline{u'v'}$ m^2/s^2	−0.0055	0.012

This problem became clearly evident in setting up our two-color TSI, back-scatter LDV. Measurements were to be made on the axis of a simple sudden expansion pipe flow where the entering mean axial velocity was about 30 m/s and turbulence intensity was 1.3%. After careful alignment of the LDV with the model and measurment of the beam convergence angles and angle of the beam planes relative to the directed flow, the measured mean radial velocity was nearly 4% of the mean axial velocity when it should have been zero.

The alignment procedure and angle measurements could not account for this magnitude of error. All angles were measured to ±0.1 deg. The alignment of the four beams was accomplished by placing a 20-μm pinhole at one of the beam waists and then making the other three beams pass through this same pinhole. With this procedure it was possible to require that the data-ready signals from the two counter processors be within 10 μs of each other and still obtain good data rates (a frequency shift of 40 MHz was used with each set of beams).

After much fruitless searching for errors, a set of data was taken using the constant time interval sampling approach of Ref. 5. A comparison of the biased and unbiased data is shown in Table 1. The radial mean velocity ($\bar{V}$) component was immediately reduced from 4% to 0.05% of the mean axial component ($\bar{U}$) with no perceptible changes to any of the other turbulence (u',v') or cross-correlation quantities ($\overline{u'v'}$), thus verifying that the problem was velocity biasing of the radial velocity component.

As more two-component LDV data become available for turbulence modeling, it becomes necessary to review carefully the method of data collection and data handling to assess its validity in even low-turbulence intensity flows. Often, sufficient details are not reported to validate the data collection and data handling procedures. Any such data should be discarded from consideration for turbulence modeling.

References

[1]McLaughlin, D. K. and Tiederman, W. G., "Bias Correction for Individual Realization Laser Anemometry Measurements in Turbulent Flows," *Physics of Fluids*, Vol. 16, No. 12, 1973, p. 2082.

[2]Roesler, T., Stevenson, W. H., and Thompson, H. D., "Investigation of Bias Errors in Laser Doppler Velocimeter Measurements," AFWAL-TR-80-2108, Dec. 1980.

[3]Stevenson, W. H., Thompson, H. D., and Luchik, T. S., "Laser Velocimeter Measurements and Analysis in Turbulent Flows with Combustion," AFWAL-TR-82-2076, Part I, Sept. 1982.

[4]Stevenson, W. H., Thompson, H. D., and Gould, R. D., "Laser Velocimeter Measurements and Analysis in Turbulent Flows with Combustion," AFWAL-TR-82-2076, Part II, July 1983.

[5]Craig, R. R., Nejad, A. S., Hahn, E. Y., "A General Approach for Obtaining Unbiased LDV Data in Highly Turbulent Non-Reacting and Reacting Flows," AIAA Paper 84-0366, Jan. 1984.

The Reduction of Pressure Drop Across a Vortex Chamber

G. H. Vatistas,* C. K. Kwok,† and S. Lin†
Concordia University, Montreal, Canada

Introduction

VORTEX chambers, in general, have a cylindrical configuration with a central axis outlet and tangential inlets. The swirling motion, imparted to the fluid by the inlet ports, generates a strong centrifugal force field and produces the complex flow pattern of Fig. 1. A common sight in vortex chambers are the two recirculatory flow areas[1,2] shown. The toroidal, eddy-type fluid motion within the chamber is of the same nature as that through a bend. The reverse flow, which takes place in the vortex core and in the vicinity of the outlet, is attributed to a local static pressure reduction to values that are below the ambient pressure P_a (where P_a is the pressure of the stagnant air ouside the chamber). The present study focuses on this reverse flow and shows, through experiments, that the pressure drop across the chamber (inlet to ambient) can be reduced by preventing the stagnant air from entering the chamber.

Experimental Apparatus

The present tests were conducted in Concordia's experimental cold cyclone furnace model. The cylindrical chamber has a constant cross-sectional area of radius R_0 of 15.24 cm (0.5 ft) and a height H of 45.72 cm (1.5 ft). Swirl is imparted to the fluid by four identical tangential inlet ports, located around the lower periphery of the chamber, 90 deg apart. The total inlet area of the ports is 68.75 cm^2 (0.074 ft^2), each port having a diameter of 4.67 cm (1.84 in.). The modular construction of the top plate incorporates several rings to allow for a variation of the exit port.

The experimental layout is schematically illustrated in Fig. 2. The volumetric flow rate is read from two variable area rotameters (not shown) connected in parallel. The static pressure drop across the chamber (inlet pressure/ambient pressure) is recorded using a sensitive well-type inclined manometer (B). The position of the conical plug is controlled with a screw-type transversing arrangement. The axial travel of the plug is read from scale A, which is graduated in 0.127 cm (0.005 in.) increments.

Results and Discussions

The effect of contraction ratio R_E/R_0 on the dimensionless pressure drop across the chamber ($\overline{\Delta P}=2(P_{\text{in}}-P_a)/\rho V_{r\text{in}}^2$) for unrestricted exit flow is presented in Fig. 3. The parameters P_{in}, ρ, and $V_{r\text{in}}$ are the static pressure at the inlet, the fluid density, and the inlet radial velocity, respectively. It is evident from Fig. 3 that $\overline{\Delta P}$ increases dramatically for small contraction ratios. Using a conical plug, one can reduce $\overline{\Delta P}$ while maintaining the same inlet flow rate Q. This is demonstrated by the experimental results given in Fig. 4. As the cone is lowered, a partial reduction of the reverse flow is achieved, which is manifested by a corresponding reduction in the static pressure drop across the chamber. When an optimum position of the cone is reached, $\overline{\Delta P}$ is at its minimum. Any further decrease of (Z/h) from the optimum results in a drastic in-

Received Dec. 6, 1983; revision received June 1, 1984.

*Ph.D. Candidate, Department of Mechanical Engineering. Member AIAA.

†Professor of Engineering, Department of Mechanical Engineering.

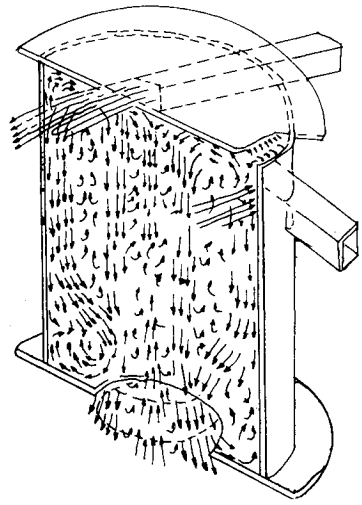

Fig. 1 Typical flow pattern in a vortex chamber (from Ref. 2).

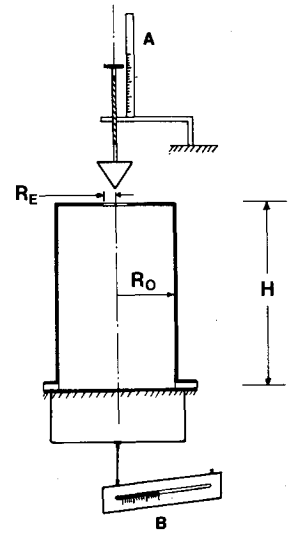

Fig. 2 Experimental apparatus.

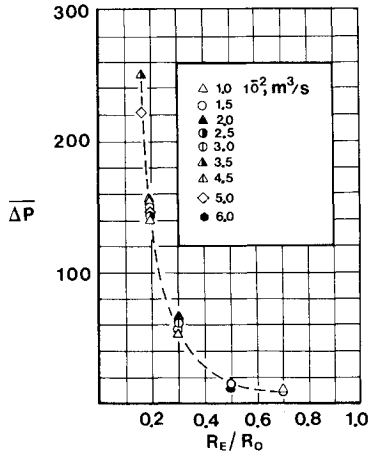

Fig. 3 Pressure drop across the chamber vs contraction ratio for different volumetric flow rates.

crease of $\overline{\Delta P}$ because the solid plug virtually covers the outlet area beyond the core. It is also worthwhile to mention that the noise level reduces considerably as the optimum position is approached. However, the noise continues to decrease below the optimum (Z/h).

The alleviation of the reverse flow through the exit with the incorporation of the conical plug was studied by means of smoke visualization. A tube with a smoke supply was placed near the centerline at a small distance above the top plate. For the condition of unrestricted exit flow, smoke is drawn into the chamber and mixes violently with the internal flow. With

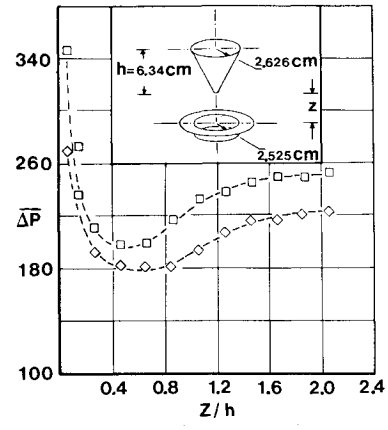

Fig. 4 Pressure drop across the chamber vs plug position (□: $Q=0.035$ m³/s; ◇: $Q=0.050$ m³/s).

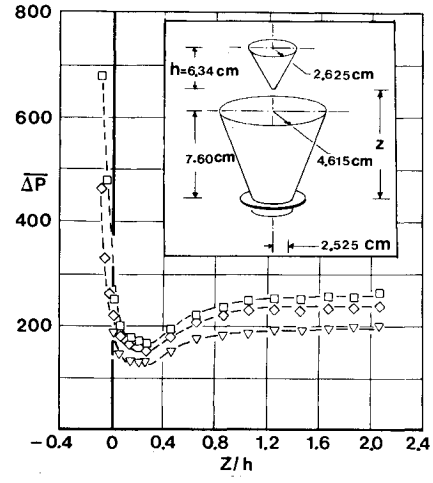

Fig. 5 Pressure drop across the chamber vs plug position with diffuser (□: $Q=0.035$ m³/s; ◇: $Q=0.050$ m³/s; ▽: $Q=0.066$ m³/s).

the plug at the optimum position, smoke supplied at the base of the cone never finds its way into the chamber. From Fig. 4, it can be seen that a 17% pressure drop reduction is possible for a contraction ratio equal to 0.16. However, the effectiveness of the plug was found to vary with R_E/R_0. For example, if R_E/R_0 is equal to 0.2, only a 5% reduction of $\overline{\Delta P}$ is possible; for 0.3, the reduction is hardly significant.

The optimum $\overline{\Delta P}$ is found to be further reduced by a combination of a conical diffuser and plug, as Fig. 5 illustrates. Although $\overline{\Delta P}$ of the unrestricted exit flow is slightly higher than that in Fig. 4, it can be seen that the percentage reduction of the pressure drop across the chamber is now approximately doubled.

Conclusions

Ways to reduce the static pressure drop across vortex chambers having small contraction ratios were presented. The reverse flow near the axis of rotation was minimized with the introduction of a conical plug. A modest reduction of static pressure drop across the chamber was obtained. A considerable pressure drop reduction was possible with a combination of a conical diffuser and plug.

References

[1]Savino, J. M. and Keshock, E. G., "Experimental Profiles of Velocity Component and Radial Pressure Distributions in a Vortex Contained in a Short Cylindrical Chamber," NASA TN D-3072, Oct. 1975.

[2]Baluev, E. D. and Troyankin, Y. V., "Study of the Aerodynamic Structure of Gas Flow in Cyclone Chambers," *Thermal Engineering*, Vol. 14, 1967, p. 99.